1.B:2.L

Nuclear Physics **A217** (1973) 14—28; © *North-Holland Publishing Co., Amsterdam*

MESON EXCHANGE CURRENTS IN DEUTERON ELECTRO-DISINTEGRATION

J. HOCKERT and D. O. RISKA †

Department of Physics, State University of New York, Stony Brook, New York 11790

M. GARI

Institut für Theoretische Physik, Ruhr Universität, Bochum, West Germany

and

A. HUFFMAN ††

Department of Physics, California Institute of Technology, Pasadena, California 91109

Received 23 July 1973

Abstract: It is shown that the impulse approximation cross section for backward ed → enp at large momentum transfer near threshold is very much smaller than the empirical data. It is found that the conventional "Jankus theory" is inadequate at large momentum transfer because of the neglect of the $^3D_1$ component of the deuteron state. By taking into account the simplest meson exchange currents of pionic range the theoretical prediction of the cross section comes into reasonable agreement with the existing data.

1. Introduction

It has long been known that meson exchange currents affect magnetic multipole transitions between different states of the neutron-proton system [1]. The apparent absence of very large discrepancies between empirical data and theoretical predictions obtained without taking into account exchange current effects has led to the general assumption that such effects give only small corrections to the transition rates. Only recently have calculations of exchange current effects become quantitatively successful in the two-nucleon system, and it has therefore been difficult to estimate their general importance. The very successful resolution by means of exchange current effects of the 10 % discrepancy between theory and experiment for the total cross section for radiative np capture $n+p \to d+\gamma$ at thermal neutron energies [2-4]) motivates a similar investigation of electron-deuteron scattering. We shall in this paper consider inelastic electron-deuteron scattering $e+d \to e+n+p$ in the backward (180°) direction near threshold. This is a reaction which has been the object of several empirical and theoretical investigations [5]). We consider this reaction in the one-photon-exchange approximation.

Near threshold the dominant nuclear transition is between the deuteron state and the $^1S_0$ np scattering state. Since this is an M1 transition it is affected by ex-

† Research supported in part by USAEC contract no. AT(11-1)-3001.

†† Supported by NSF GP-28027.

change currents, and thus will provide information on the importance of such effects. For backward scattering there is no contribution to the cross section from the Coulomb and Darwin-Foldy terms in the interaction, and thus the M1 transition to the $^1S_0$ state dominates the reaction over a relatively wide range of the low energy region.

We first re-evaluate the backward differential cross section in the impulse approximation; i.e., neglecting exchange current effects. We find that at large values of momentum transfer the $^3D_1$ component of the deuteron state is very important. This component is neglected in the usual "Jankus theory" [6]) treatment of e+d → e+n+p, and therefore the "Jankus theory" is inadequate for momentum transfer values $\gtrsim 1\ \text{fm}^{-1}$. The correct impulse approximation prediction for the cross section is very much smaller than the empirical results. We demonstrate that most of this discrepancy can be removed by taking into account the simplest meson exchange current processes of pionic range. We take into account the same meson exchange processes as were taken into account in ref. [2]).

The only previous work in this direction is that of Adler [7]). In that work some exchange current processes of less importance than those considered in the present work were taken into account. Some of the conclusions of ref. [7]) were distorted because of incorrect expressions for the cross sections. We shall nevertheless use the notation of Adler as far as possible.

We divide this paper into four sections. In sect. 2 we rederive the impulse approximation cross section for backward e+d → e+n+p. In sect. 3 we derive the contributions to the cross section due to the exchange currents of pionic range. In sect. 4 we give the numerical results and a concluding discussion.

2. Impulse approximation

In this section we give a brief review of the calculation of the impulse approximation cross section for the reaction e+d → e+n+p. Our aim is to emphasize the importance of $^3D_1$ component of the deuteron state. We refer to refs. [5, 6]) for a complete exposition of the conventional "Jankus theory" treatment in which the $^3D_1$ component is neglected.

In the one-photon exchange approximation the differential cross section near threshold may be expressed in terms of the matrix elements of the electromagnetic (e.m.) current of the np system [5]) as

$$\frac{\mathrm{d}\sigma}{\mathrm{d}k'\mathrm{d}\Omega} = \frac{mp\sigma_{\mathrm{M}}}{8\pi^2}\{[\varepsilon'_\mu \varepsilon_\nu + \varepsilon'_\nu \varepsilon_\mu] \sec^2 \tfrac{1}{2}\theta + 2\delta_{\mu\nu} \tan^2 \tfrac{1}{2}\theta\} J^*_\mu J_\nu . \tag{2.1}$$

Here m is the nucleon mass, p the momentum of the final proton in the c.m. system of the two nucleons and θ the electron scattering angle. We have defined $\varepsilon_\mu = k_\mu/k$ and $\varepsilon'_\mu = k'_\mu/k'$, where k_μ, k'_μ are the four-momenta of the initial and final electrons respectively. The corresponding electron energies are k, k'. The Mott cross section is

$$\sigma_M = (\alpha^2/4k^2)\cos^2 \tfrac{1}{2}\theta \sin^{-4} \tfrac{1}{2}\theta, \tag{2.2}$$

where α is the fine structure constant. The matrix element of the e.m. current operator of the np system is defined as

$$J_\mu = \int d^3x\, d^3y\, \phi_f^*(\boldsymbol{x}, \boldsymbol{y}) J_\mu(\boldsymbol{x}, \boldsymbol{y}) \phi_i(\boldsymbol{x}, \boldsymbol{y}). \tag{2.3}$$

Here ϕ_i and ϕ_f are the wave functions describing the deuteron state and the final np scattering state respectively. By factoring out the c.m. motion and going over to a momentum space representation, we may rewrite the expression for the matrix element as

$$J_\mu = \int d^3r\, \phi_f^*(\boldsymbol{r}) \int \frac{d^3\tau}{(2\pi)^3}\, e^{i\tau\cdot \boldsymbol{r}} \tilde{J}_\mu(\tfrac{1}{2}\boldsymbol{q}+\tau, \tfrac{1}{2}\boldsymbol{q}-\tau)\phi_i(\boldsymbol{r}). \tag{2.4}$$

Here $\boldsymbol{q}$ is the momentum transfer from the electron. The Fourier transform of the current operator is defined by

$$J_\mu(\boldsymbol{x}, \boldsymbol{y}) = (2\pi)^{-6} \int d^3k\, d^3l\, e^{i\boldsymbol{k}\cdot\boldsymbol{x} + i\boldsymbol{l}\cdot\boldsymbol{y}} \tilde{J}_\mu(\boldsymbol{k}, \boldsymbol{l}). \tag{2.5}$$

In the impulse approximation it is assumed that the total momentum transferred is delivered to either one of the nucleons without subsequent exchange of mesons. In this case $\tilde{J}_\mu$ can be decomposed into a sum of single nucleon currents as

$$\tilde{J}_\mu^{\text{imp}} = (2\pi)^3\{\delta(\tfrac{1}{2}\boldsymbol{q}-\tau)\tilde{J}_\mu^{(1)}(\boldsymbol{q}) + \delta(\tfrac{1}{2}\boldsymbol{q}+\tau)\tilde{J}_\mu^{(2)}(\boldsymbol{q})\}. \tag{2.6}$$

The covariant expression for the single nucleon current $\tilde{J}_\mu^{(j)}$ is

$$\langle p'|\tilde{J}_\mu^{(j)}|p\rangle = i\bar{u}(p')[\underset{\sim}{F}_1^{(j)}\gamma_\mu^{(j)} - \underset{\sim}{F}_2^{(j)}\sigma_{\mu\nu}^{(j)}q_\nu]u(p), \tag{2.7}$$

with $q = p'-p$.

The isospin operators $\underset{\sim}{F}_{1,2}^{(j)}$ have the following decomposition in terms of form factors:

$$\underset{\sim}{F}_{1,2}^{(j)} = \tfrac{1}{2}[F_{1,2}^{S}(q^2) + \tau_3^{(j)}F_{1,2}^{V}(q^2)]. \tag{2.8}$$

The noncovariant expansion of $\tilde{J}_\mu^{(j)}$ valid to second order in $\boldsymbol{q}$ and first order in $\boldsymbol{P} = \tfrac{1}{2}(\boldsymbol{p}'+\boldsymbol{p})$ is

$$J_0^{(j)} = \underset{\sim}{G}_E^{(j)}(q^2), \tag{2.9a}$$

$$\boldsymbol{J}^{(j)} = \frac{1}{m}\underset{\sim}{F}_1^{(j)}\boldsymbol{P}^{(j)} + \frac{i}{2m}\underset{\sim}{G}_M^{(j)}(q^2)\boldsymbol{\sigma}^{(j)}\times\boldsymbol{q}. \tag{2.9b}$$

Here we have defined the form factors $\underset{\sim}{G}(q^2)$ as

$$\underset{\sim}{G}_E(q^2) = \underset{\sim}{F}_1(q^2) - \frac{\boldsymbol{q}^2}{2m}\underset{\sim}{F}_2(q^2),$$

$$\underset{\sim}{G}_M(q^2) = \underset{\sim}{F}_1(q^2) + 2m\underset{\sim}{F}_2(q^2). \tag{2.10}$$

In the following we shall not distinguish between q^2 and $\boldsymbol{q}^2$ since for $\theta = 180°$, $\boldsymbol{q}^2 - q^2 = (k-k')^2$ which is a small number near threshold.

The radial part of the wave function for the deuteron is

$$\phi_i(\boldsymbol{r}) = \frac{1}{\sqrt{4\pi}}\left(\frac{u(r)}{r} + \frac{w(r)}{r}\frac{S_{12}}{\sqrt{8}}\right), \tag{2.11}$$

where $S_{12} = 3(\boldsymbol{\sigma}^1 \cdot \hat{\boldsymbol{r}})(\boldsymbol{\sigma}^2 \cdot \hat{\boldsymbol{r}}) - \boldsymbol{\sigma}^1 \cdot \boldsymbol{\sigma}^2$. We shall consider energies so close to threshold that only the S-wave components of the final scattering state are important. Since the cross section is the sum of the cross sections for transitions to singlet and triplet spin states we may consider these partial cross section separately.

Consider first the transitions to the final $^1S_0$ state. Neglecting the unimportant phase factor, we may write the final $^1S_0$ state wave function as

$$\phi_f(\boldsymbol{r}) = \frac{1}{pr} F_{000}(pr), \tag{2.12}$$

where $F_{000}(pr) \to \sin(pr + \delta_{000})$ when $r \to \infty$. The general notation for the radial wave functions and phase shifts in the uncoupled states is F_{JLS} and δ_{JLS}.

Only the magnetic spin current term in (2.9b) causes triplet to singlet transitions. By inserting this term of the e.m. current in (2.6) and (2.4), one finds that the radial matrix element of the current has the form

$$\boldsymbol{J} = i\frac{\sqrt{\pi}}{2m}\{g(q^2)[-i\boldsymbol{\sigma}^1 \times \boldsymbol{\sigma}^2] + h(q^2)(\boldsymbol{\sigma}^1 - \boldsymbol{\sigma}^2)\} \times \boldsymbol{q}. \tag{2.13}$$

The impulse approximation results for the functions g and h are

$$g^{\text{imp}}(q^2) = -G_M^V(q^2)J_S(q^2), \tag{2.14}$$
$$h^{\text{imp}}(q^2) = G_M^V(q^2)[H_S(q^2) - J_S(q^2)].$$

The functions H_S and J_S are defined as in ref. [7]) as

$$H_S(q^2) = (1/p)\int_0^\infty \mathrm{d}r\, F_{000}(pr) j_0(\tfrac{1}{2}qr)u(r),$$

$$J_S(q^2) = (1/p\sqrt{8})\int_0^\infty \mathrm{d}r\, F_{000}(pr) j_2(\tfrac{1}{2}qr)w(r). \tag{2.15}$$

To compute the unpolarized cross section in (2.1) one has to sum over the final and average over the initial spin directions. Carrying out this procedure one obtains for the differential cross section for 180° scattering to the $^1S_0$ state the expression†

$$\left(\frac{\mathrm{d}\sigma}{\mathrm{d}k'\mathrm{d}\Omega}\right)_{^1S_0} = \frac{\alpha^2}{24\pi}\frac{pq^2}{mk^2}[g(q^2) + h(q^2)]^2. \tag{2.16}$$

† The expression for the cross section is incorrectly given in ref. [7]).

The impulse approximation cross section is thus proportional to the quantity $(H_S - 2J_S)^2$ (neglecting other final states than $^1S_0$). The "Jankus theory" approximation amounts to neglecting J_S in the bracket. This is clearly justified for very small values of q^2 since $J_S \xrightarrow[q^2\to 0]{} 0$. However for $q^2 > 1\ \mathrm{fm}^{-2}$, J_S becomes an appreciable fraction of H_S and this approximation becomes invalid. This is illustrated in fig. 2 where we have plotted the structure functions H_S and J_S for $E_{\mathrm{c.m.}} = 3$ MeV kinetic energy in the c.m.s. of the final np state. The consequence of the destructive interference between H_S and J_S is to predict a sharp minimum in the cross section which has not been seen experimentally.

The cross section for transitions to the scattering state $^3S_1 + {}^3D_1$, the main component of which corresponds to $^3S_1$ ("α-state") is somewhat more complicated to calculate. However the $^3D_1$ component of the α-state does not play a large role in transitions between the deuteron bound state and the α-state, because the cross section is an incoherent sum of contributions and not a coherent sum as in the transition to the final $^1S_0$ state. If we neglect the $^3D_1$ admixture of the α-state, the remaining $^3S_1$ wave function is

$$\phi_f(r) = (1/pr)F_{101}(pr), \tag{2.17}$$

where $F_{101}(pr) \xrightarrow[r\to\infty]{} \sin(pr + \delta_{101})$ with δ_{101} being the eigenphase shift of the α-state.

The general expression for the radial matrix element of the current in this case may be written in the form†

$$\boldsymbol{J} = i\frac{\sqrt{\pi}}{2m}\{j(q^2)(\boldsymbol{\sigma}^1 + \boldsymbol{\sigma}^2) + k(q^2)\boldsymbol{\Sigma}_{12}\} \times \boldsymbol{q}. \tag{2.18}$$

We define $\boldsymbol{\Sigma}_{12}$ as

$$\boldsymbol{\Sigma}_{12} = i[(\boldsymbol{\sigma}^1 \times \hat{\boldsymbol{q}})(\boldsymbol{\sigma}^2 \cdot \hat{\boldsymbol{q}}) + (\boldsymbol{\sigma}^2 \times \hat{\boldsymbol{q}})(\boldsymbol{\sigma}^1 \cdot \hat{\boldsymbol{q}})]. \tag{2.19}$$

All the terms in the e.m. current in (2.9) contribute to the $(^3S_1 + {}^3D_1)$ transition. However the Coulomb and Darwin-Foldy parts (J_0) do not contribute at $\theta = 180°$. The contributions to the form factors j and k in (2.18) due to the convection and magnetic spin currents in (2.9b) are

$$\begin{aligned} j(q^2) &= G_M^S(q^2)(H_t(q^2) + J_t(q^2)), \\ k(q^2) &= 3[G_M^S(q^2)J_t(q^2) - 8F_1^S(q^2)K_t(q^2)]. \end{aligned} \tag{2.20}$$

Here we have used the notation of Adler [7]) for the structure functions H_t, J_t and K_t:

$$H_t(q^2) = \frac{1}{p}\int_0^\infty \mathrm{d}r\, F_{101}(pr) j_0(\tfrac{1}{2}qr)u(r), \tag{2.21a}$$

$$J_t(q^2) = \frac{1}{p\sqrt{8}}\int_0^\infty \mathrm{d}r\, F_{101}(pr) j_2(\tfrac{1}{2}qr)w(r), \tag{2.21b}$$

$$K_t(q^2) = \frac{1}{p\sqrt{8}}\int_0^\infty \mathrm{d}r \left(\frac{rF'_{101} - F_{101}}{r^2q^2}\right) j_2(\tfrac{1}{2}qr)w(r). \tag{2.21c}$$

† The electric contributions to the current which do not contribute to 180° scattering do not have this form.

In the derivation of the convection current contributions (2.21c) we have used the fact that the momentum vector $\boldsymbol{P}^{(j)}$ in (2.9b) may be interpreted as a gradient operator on the final wave function. This is possible in the laboratory frame in which the target deuteron is at rest.

By again averaging over the initial and summing over the final spin directions we obtain the differential cross section for 180° scattering in the form

$$\left(\frac{\mathrm{d}\sigma}{\mathrm{d}k'\mathrm{d}\Omega}\right)_{^3\mathrm{S}_1} = \frac{\alpha^2}{12\pi}\left(\frac{p}{m}\right)\frac{q^2}{k^2}(j^2(q^2)+k^2(q^2)). \tag{2.22}$$

The total differential cross section is the sum of the expressions (2.16) and (2.22). The cross section to the $^3\mathrm{S}_1$ state is very small compared to the cross section to the $^1\mathrm{S}_0$ state at low values of momentum transfer because of the near orthogonality of the bound and free $^3\mathrm{S}_1$ states, and because the isoscalar magnetic form factor is much smaller than the isovector one.

3. Meson exchange currents

The meson exchange processes of longest range are shown in fig. 1. There is, of course, no limit to the number of possible contributing exchange current processes,

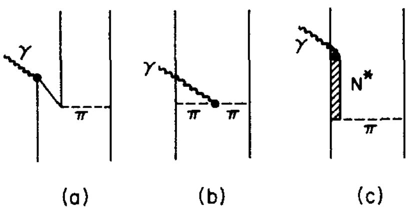

Fig. 1. Exchange current processes contributing to e+d → e+n+p: (a) pair excitation process; (b) pion current process; (c) resonance excitation process.

but only those of pionic range are very significant, since short range heavy meson exchange processes are suppressed by the strong short range repulsion in the nucleon-nucleon interaction. We shall only take into account the processes shown in fig. 1, since the inclusion of those processes led to excellent agreement between the theoretical and empirical values for the total cross section for the related process n+p → d+γ at thermal neutron energies [2]). The transition operators representing these exchange current processes all have isovector character, and do therefore lead to transitions from the deuteron state to the final $^1\mathrm{S}_0$ state but not to the α state.

The most important exchange current process is the pair excitation process in fig. 1a. The two-nucleon current operator due to this process is

$$j^{\mathrm{pair}}(\boldsymbol{k}, \boldsymbol{l}) = \frac{ig^2}{4m^2}F_1^{\mathrm{V}}(q^2)(\boldsymbol{\tau}^1\times\boldsymbol{\tau}^2)_3\left[\frac{\boldsymbol{\sigma}^2(\boldsymbol{\sigma}^1\cdot\boldsymbol{k})}{\mu^2+k^2}-\frac{\boldsymbol{\sigma}^1(\boldsymbol{\sigma}^2\cdot\boldsymbol{l})}{\mu^2+l^2}\right]. \tag{3.1}$$

Here $g^2/4\pi = 14.5$ is the usual pseudoscalar πN coupling constant. We have used the usual nucleon e.m. form factor $F_1^V(q^2)$, which strictly applies only for the case of nucleons on mass shell. However, the same form factor is used in the impulse approximation expression regardless of the fact that the nucleons bound in the deuteron are off mass shell. The contributions to the form factors g and h in (2.13) and (2.16) due to the pair excitation current (3.1) are

$$g^{\text{pair}}(q^2) = 2\left(\frac{g^2}{4\pi}\right)\left(\frac{\mu}{m}\right)[K^1(q^2)+K^2(q^2)], \tag{3.2}$$

$$h^{\text{pair}}(q^2) = 2\left(\frac{g^2}{4\pi}\right)\left(\frac{\mu}{m}\right)K^2(q^2). \tag{3.3}$$

The structure functions K in (3.3) are defined as

$$K^1(q^2) = \frac{\mu}{qp}\int_0^\infty \mathrm{d}r\, F_{000}(pr)j_1(\tfrac{1}{2}qr)\frac{Y_1(\mu r)}{\mu r}u(r),$$

$$K^2(q^2) = \frac{\mu}{qp\sqrt{8}}\int_0^\infty \mathrm{d}r\, F_{000}(pr)j_1(\tfrac{1}{2}qr)\frac{Y_1(\mu r)}{\mu r}w(r). \tag{3.4}$$

Here $Y_1(x) = (1+x)\mathrm{e}^{-x}/x$.

The two-nucleon current due to the pion exchange current in fig. 1b has the form

$$J^\pi(\boldsymbol{k}, \boldsymbol{l}) = \frac{ig^2}{4m^2}F_\pi(q^2)(\boldsymbol{\tau}^1\times\boldsymbol{\tau}^2)_3\frac{(\boldsymbol{k}-\boldsymbol{l})(\boldsymbol{\sigma}^1\cdot\boldsymbol{k})(\boldsymbol{\sigma}^2\cdot\boldsymbol{l})}{(\mu^2+k^2)(\mu^2+l^2)}. \tag{3.5}$$

Here $F_\pi(q^2)$ is the pion e.m. form factor. The contributions from the pionic current process to the form factors g, h are†

$$g^\pi(q^2) = \frac{g^2}{16m}[\zeta(q^2)-\eta(q^2)]F_\pi(q^2),$$

$$h^\pi(q^2) = \frac{g^2}{16m}\zeta(q^2)F_\pi(q^2). \tag{3.6}$$

We define the structure functions η, ζ as in ref. [7]) by

$$\eta(q^2) = (1/8\pi^2)\int_0^\infty \mathrm{d}\tau\,\tau^4 H_S(\tau^2)M(\tau, q),$$

$$\zeta(q^2) = (1/8\pi^2)\int_0^\infty \mathrm{d}\tau\,\tau^4 J_S(\tau^2)M(\tau, q). \tag{3.7}$$

The auxiliary function $M(\tau, q)$ is defined as

$$M(\tau, q) = \frac{8}{q^2\tau^2}+\frac{2[(q^2+\tau^2+4\mu^2)^2-4q^2\tau^2]}{q^3\tau^3(q^2+\tau^2+4\mu^2)}\log\left(\frac{4\mu^2}{4\mu^2+q^2+\tau^2+2q\tau}\,\frac{q^2+\tau^2-2q\tau}{}\right). \tag{3.8}$$

† The sign of the function g^π is incorrect in ref. [7]).

We finally consider the πN rescattering effect shown in fig. 1c. There are many approaches to the evaluation of this effect. We shall here use the static quark model and assume $\Delta_{33}(1236)$ dominance, and use the sharp resonance approximation. In fact the results do not change much if one instead uses the dispersion theoretical results of Chemtob and Rho [8]), or the Chew-Low model [9]) with the Δ_{33} dominance assumption. In the approach of Chemtob and Rho the effect of the $N'_{11}(1470)$ resonance is included but we have found its influence to be negligible. The main problem is the question of the γNΔ_{33} vertex at large values of momentum transfer. We shall here simply assume that the ratio between this vertex function and the corresponding γNN vertex function is a constant given by the static quark model. This is probably the simplest possible ansatz for the extrapolation to large q^2.

In the static quark model the exchange current due to the Δ_{33} resonance is

$$\tilde{J}^{\Delta}(\boldsymbol{k}, \boldsymbol{l}) = \frac{ig^2 G_M^V(q^2)}{25m^3(m^*-m)} \left\{ 4\tau_3^1 \frac{(\boldsymbol{k}\times\boldsymbol{q})(\boldsymbol{\sigma}^1\cdot\boldsymbol{k})}{\mu^2+k^2} + 4\tau_3^2 \frac{(\boldsymbol{l}\times\boldsymbol{q})(\boldsymbol{\sigma}^2\cdot\boldsymbol{l})}{\mu^2+l^2} - (\boldsymbol{\tau}^1\times\boldsymbol{\tau}^2)_3 \left[\frac{(\boldsymbol{\sigma}^1\times\boldsymbol{l})\times\boldsymbol{q}(\boldsymbol{\sigma}^2\cdot\boldsymbol{l})}{\mu^2+l^2} - \frac{(\boldsymbol{\sigma}^2\times\boldsymbol{k})\times\boldsymbol{q}(\boldsymbol{\sigma}^1\cdot\boldsymbol{k})}{\mu^2+k^2} \right] \right\}. \tag{3.9}$$

Here $m^* = 1236$ MeV is the mass of the Δ_{33} resonance. The contributions due to this current to the form factors g, h are

$$g^{\Delta}(q^2) = \tfrac{1}{12}\xi\{3K^3 - K^4 + 6K^5 + 2K^6\},$$
$$h^{\Delta}(q^2) = \tfrac{1}{12}\xi\{3K^3 - 2K^4 + 6K^5 - 2K^6\}. \tag{3.10}$$

We have here defined

$$\xi = \frac{32}{25}\left(\frac{f^2}{4\pi}\right)\frac{\mu}{m^*-m}\,G_M^V(q^2). \tag{3.11}$$

The structure functions K are defined as

$$K^3(q^2) = \frac{1}{p\sqrt{8}}\int_0^\infty \mathrm{d}r\, F_{000}(pr) j_2(\tfrac{1}{2}qr) Y_2(\mu r) w(r),$$
$$K^4(q^2) = \frac{1}{p}\int_0^\infty \mathrm{d}r\, F_{000}(pr) j_2(\tfrac{1}{2}qr) Y_2(\mu r) u(r),$$
$$K^5(q^2) = \frac{1}{p\sqrt{8}}\int_0^\infty \mathrm{d}r\, F_{000}(pr) j_0(\tfrac{1}{2}qr) Y_2(\mu r) w(r),$$
$$K^6(q^2) = \frac{1}{p}\int_0^\infty \mathrm{d}r\, F_{000}(pr) j_0(\tfrac{1}{2}qr) Y_0(\mu r) u(r). \tag{3.12}$$

We have used the notation [8])

$$Y_0(x) = \frac{e^{-x}}{x}, \qquad Y_2(x) = \left(\frac{3}{x^2} + \frac{3}{x} + 1\right)\frac{e^{-x}}{x}. \tag{3.13}$$

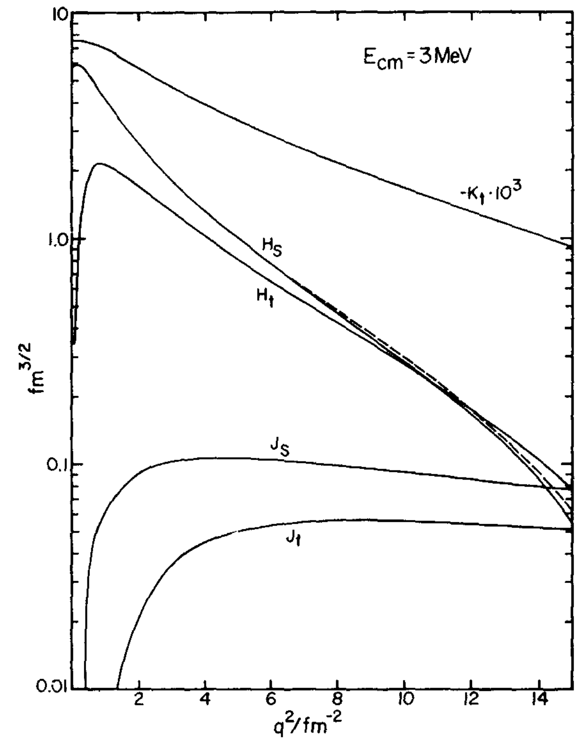

Fig. 2. Structure functions for the impulse approximation corresponding to $E_{c.m.} = 3$ MeV. The solid lines correspond to the results obtained with wave functions obtained with the Reid hard core potential. The dotted line shows H_S when instead the Reid soft core potential is used. Both potentials give almost identical results for J_S.

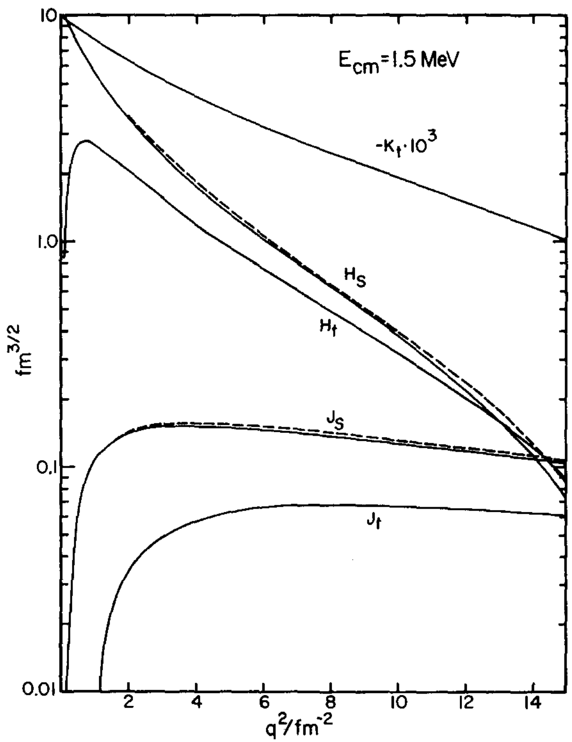

Fig. 3. Structure functions for the impulse approximation corresponding to $E_{c.m.} = 1.5$ MeV. The notation is the same as in fig. 2.

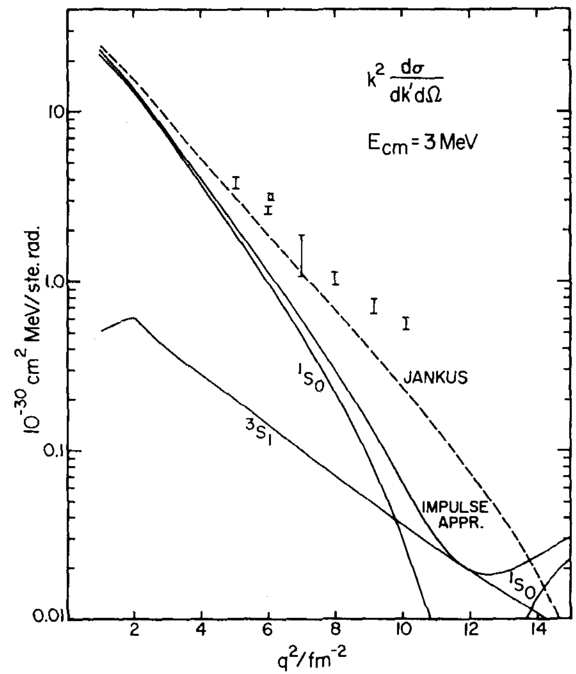

Fig. 4. The impulse approximation cross section for $E_{c.m.} = 3$ MeV. The cross section has been multiplied by the square of the incident electron energy. The difference between the correct impulse approximation result and the Jankus theory result is due to the effect of the $^3D_1$ component of the deuteron. The partial cross sections for transitions to $^1S_0$ and $^3S_1$ scattering states are denoted $^1S_0$ and $^3S_1$. The data are from ref. [11]), except for the point marked by a circle which is taken from ref. [12]).

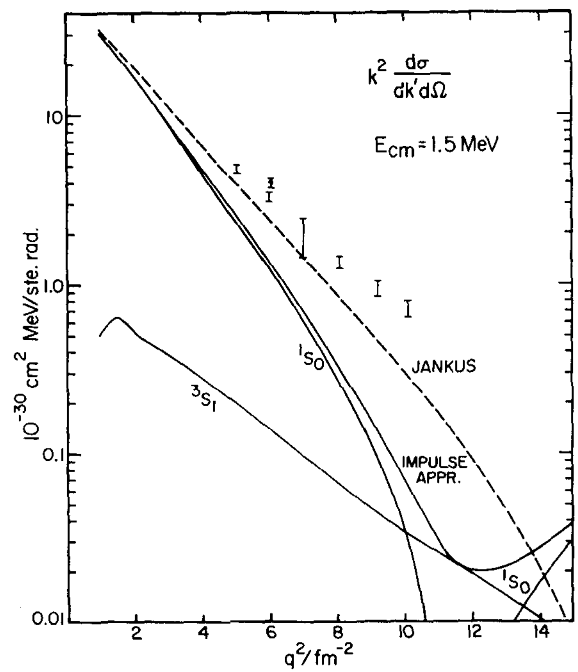

Fig. 5. The impulse approximation cross section for $E_{c.m.} = 1.5$ MeV. The notation is the same as in fig. 4.

There is another exchange current process of pionic range, namely the process in which the photon excites the exchanged pion to an ω-meson. The contribution of this process is however small compared to that of the Δ_{33} resonance [2]). We do not include it here.

4. Numerical results

We have computed the impulse approximation structure functions H_S and J_S for $E_{c.m.} = 1.5$ and 3 MeV. The results are exhibited in figs. 2 and 3. We used the wave functions for the deuteron and the $^1S_0$ scattering state obtained by solving the Schrödinger equation with the Reid hard core and soft core potentials [10]). Both sets of wave functions give almost identical results for the structure functions. Because of the destructive interference between H_S and J_S the impulse approximation cross section for the $^1S_0$ state will have a sharp minimum for $q^2 \approx 12\ \mathrm{fm}^{-2}$.

In figs. 2 and 3 we have also plotted the structure functions H_t, J_t and K_t describing the transition to the $^3S_1$ scattering state. These were computed with wave functions corresponding to the Reid hard core potential.

The impulse approximation cross section is plotted in figs. 4 and 5 for $E_{c.m.} = 3$ and 1.5 MeV respectively. We have multiplied the cross section by k^2 to get rid of the dependence on the incident electron energy. The effect of the $^3D_1$ component of the deuteron on the cross section to the $^1S_0$ state is demonstrated by the difference between the curves Jankus and $^1S_0$ which represent the $^1S_0$ cross section calculated without and with the $^3D_1$ component in the wave function. The results Jankus are thus the results of "Jankus theory". The relative unimportance of the transition to the final $^3S_1$ state is evident.

The data points are taken from refs. [11, 12]). Since in those references the data were given in terms of a constant coefficient by which the "Jankus theory" result should be multiplied to agree with the empirical data in the energy region near threshold, the "data" in the figures were obtained by multiplying our Jankus theory results by the given coefficient. Since in refs. [11, 12]) the wave functions used in the "Jankus theory" expressions were different from the wave functions we use, the "data" points in the figures should not be taken too literally. We have furthermore divided all the data points by the radiative correction factor 0.92 used by Adler [7]), rather than, as he did, multiply the theoretical values by that factor. For low values of momentum transfer a cavalier treatment of the data of this kind is not necessary (rather it would be inexcusable) because of the existence of tabulated data, for which the radiative corrections have been taken into account [12]).

In computing the cross sections we used the dipole five-parameter fits for the nucleon e.m. form factors given in ref. [13]).

It is interesting to note the very big discrepancy between the data and the impulse approximation cross section. A straight extrapolation of the data does not seem to support the impulse approximation prediction of a minimum in the cross section at

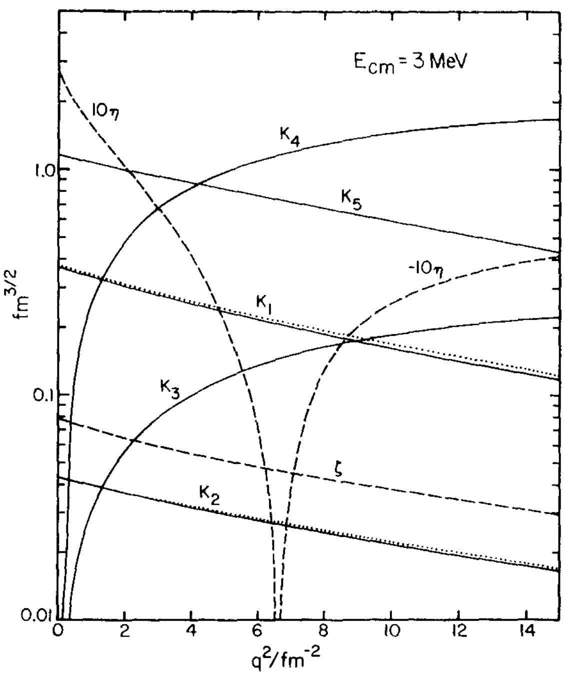

Fig. 6. Structure functions associated with the exchange current contributions for $E_{c.m.} = 3$ MeV. The units of all functions are $fm^{\frac{3}{2}}$ except η and ζ which have $fm^{\frac{1}{2}}$.

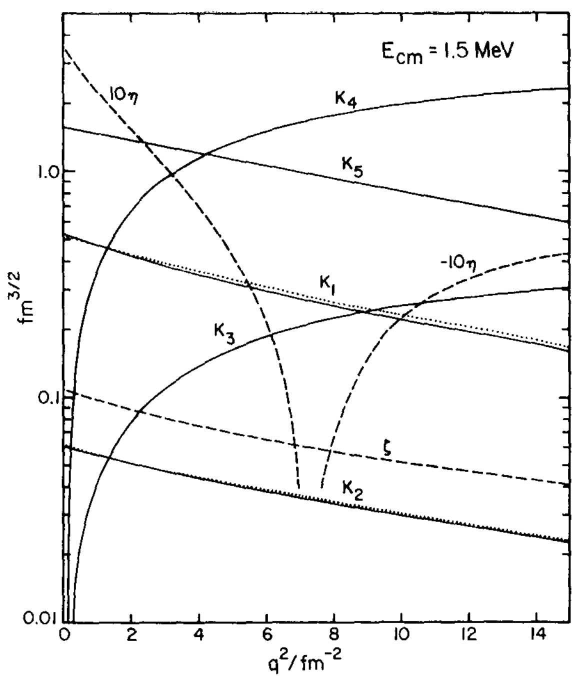

Fig. 7. Structure functions associated with the exchange contributions for $E_{c.m.} = 1.5$ MeV. The units of all functions are $fm^{\frac{3}{2}}$ except η and ζ which have $fm^{\frac{1}{2}}$.

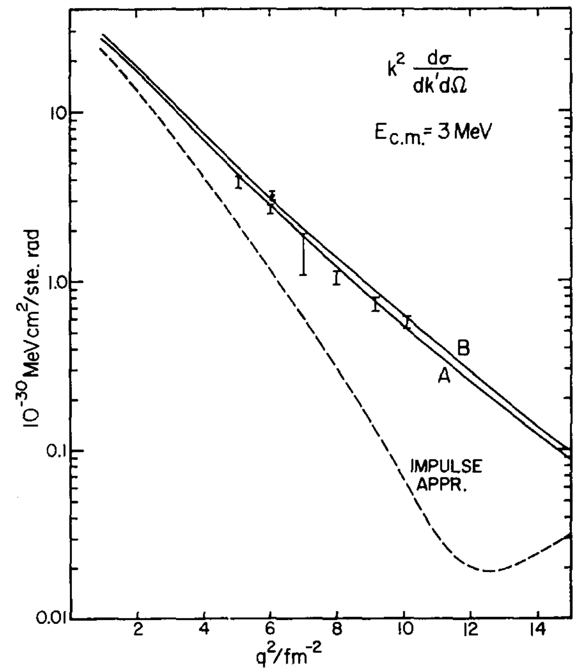

Fig. 8. Cross section for $E_{c.m.} = 3$ MeV. The curve A shows the cross section when the pion and pair processes are taken into account and the curve B when also the Δ_{33} resonance contribution is included. The data points are the same as in fig. 4.

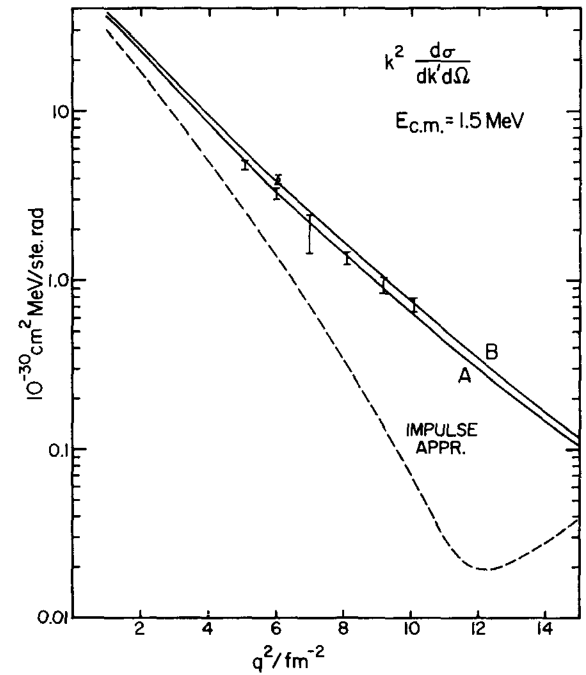

Fig. 9. The cross section for $E_{c.m.} = 1.5$ MeV. The notation is the same as in fig. 8.

$q^2 \approx 12\ \text{fm}^{-2}$. It would be very important that the cross section measurements be extended to this region of momentum transfer since the cross section in this region will mainly be built up by exchange current effects.

In figs. 6 and 7 we have plotted the structure functions associated with the exchange current processes discussed in sect. 3. The most important structure functions are K^1 and K^2 associated with the pair excitation current. The fact that K^1 decreases more slowly with increasing q^2 than H_S means that the exchange current processes gain in importance with increasing q^2. In figs. 8 and 9 we have plotted the cross section predicted when the exchange currents are taken into account. In computing the pionic exchange current we used the pion e.m. form factor of ref. [14]). The curves A represent the cross section when the pionic and pair excitation currents are taken into account. In this result the pionic current plays a minor role in comparison with the pair excitation current. The curves B show the cross section when in addition the Δ_{33} resonance is included.

Both the curves A and B are in qualitative agreement with the data in the figures. Because of our cavalier treatment of the data it is not possible to draw very strong conclusions based on this fact. However the fact that the theoretical results do not differ by orders of magnitude from the empirical ones does demonstrate the following points: (i) "Jankus theory" gives an inadequate description for $q^2 > 1\ \text{fm}^{-2}$, (ii) the impulse approximation cross section is very much smaller than the empirical results, and (iii) exchange currents are very important at large momentum transfer.

All theoretical results in this paper have an intrinsic $\pm 10\,\%$ uncertainty arising from the fact that in the nonrelativistic reduction of the e.m. current we have neglected terms of the order $q^2/4m^2$ in comparison to 1. Due to uncertainties in the nuclear wave functions additional inaccuracies of perhaps the same order of magnitude must be admitted. As far as the exchange currents are concerned, the expressions for the pair excitation and pion currents are unambiguous (to terms of order $q^2/4m^2$). A more careful treatment of the rescattering effects may change the cross section results (B) somewhat. Finally we did not take into account the scattering to ^{3}P states. The effect of the $^3\text{D}_1$ component of the α-state on the cross section was found to be negligible.

One of us (D.O.R.) wishes to thank Professors G. E. Brown, W. D. Turchinetz, R. J. Adler and B. Chertok for their interest in this work and for some stimulating discussions, and Prof. P. Signell for allowing the use of a computer code for solving the Schrödinger equation developed at Michigan State University.

References

1) N. Austern and E. Rost, Phys. Rev. **117** (1959) 1506
2) D. O. Riska and G. E. Brown, Phys. Lett. **38B** (1972) 193
3) M. Gari and A. Huffman, Phys. Rev. **C7** (1973) 994
4) J. Thakur and L. L. Foldy, Case Western Reserve Univ. preprint 1973

5) T. A. Griffy and L. I. Schiff, High energy physics, vol. 1, ed. E. H. S. Burhop (Academic Press, New York, 1967) p. 341
6) V. Z. Jankus, Phys. Rev. **102** (1956) 1586;
L. Durand III, Phys. Rev. **123** (1961) 1393
7) R. J. Adler, Phys. Rev. **169** (1968) 1192
8) M. Chemtob and M. Rho, Nucl. Phys. **A163** (1971) 1
9) G. F. Chew and F. E. Low, Phys. Rev. **101** (1956) 1570
10) R. V. Reid, Ann. of Phys. **50** (1968) 411
11) R. E. Rand *et al.*, Phys. Rev. Lett. **18** (1967) 469
12) D. Ganichot, D. Grossetête and D. B. Isabelle, Nucl. Phys. **A178** (1972) 545
13) F. Iachello, A. D. Jackson and A. Lande, Phys. Lett. **43B** (1973) 191
14) M. Roos and J. Pišút, Nucl. Phys. **B10** (1969) 563